The University of Southern Mississippi

The Aquila Digital Community

Faculty Publications

9-19-2016

A New Class of Allosteric HIV-1 Integrase Inhibitors Identified by Crstallographic Fragment Screening of the Catalytic Core Domain

Disha Patel
Rutgers University

Janet Antwi
Ohio State University

Pratibha C. Koneru
Ohio State University

Erik Serrao
Harvard Medical School

Stefano Forli
The Scripps Research Institute

See next page for additional authors

Follow this and additional works at: https://aquila.usm.edu/fac_pubs

Part of the Chemistry Commons

Authors

Disha Patel, Janet Antwi, Pratibha C. Koneru, Erik Serrao, Stefano Forli, Jacques J. Kessl, Lei Feng, Nanjie Deng, Ronald M. Levy, James R. Fuchs, Arthur J. Olson, Alan N. Engelman, Joseph D. Bauman, Mamuka Kvaratskhelia, and Eddy Arnold

A New Class of Allosteric HIV-1 Integrase Inhibitors Identified by Crystallographic Fragment Screening of the Catalytic Core Domain*[S]

Disha Patel[‡], Janet Antwi[§], Pratibha C. Koneru[¶], Erik Serrao[‖], Stefano Forli[**], Jacques J. Kessl[‡‡], Lei Feng[¶], Nanjie Deng[§§], Ronald M. Levy[§§], James R. Fuchs[§], Arthur J. Olson[**], Alan N. Engelman[‖], Joseph D. Bauman[‡], Mamuka Kvaratskhelia[¶1], and Eddy Arnold[‡2]

From the [‡]Center for Advanced Biotechnology and Medicine, Rutgers University, Piscataway, New Jersey 08854, [§]Division of Medicinal Chemistry and Pharmacognosy, College of Pharmacy and [¶]Center for Retrovirus Research and College of Pharmacy, Ohio State University, Columbus, Ohio 43210, [‖]Department of Cancer Immunology and Virology, Dana-Farber Cancer Institute and Department of Medicine, Harvard Medical School, Boston, Massachusetts 02215, [**]Molecular Graphics Laboratory, Department of Integrative Structural and Computational Biology, MB-112, The Scripps Research Institute, La Jolla, California 92037, [‡‡]Department of Chemistry and Biochemistry, University of Southern Mississippi, Hattiesburg, Mississippi 39406, and [§§]Center for Biophysics and Computational Biology, Temple University, Philadelphia, Pennsylvania 19122

Edited by Norma Allewell

HIV-1 integrase (IN) is essential for virus replication and represents an important multifunctional therapeutic target. Recently discovered quinoline-based allosteric IN inhibitors (ALLINIs) potently impair HIV-1 replication and are currently in clinical trials. ALLINIs exhibit a multimodal mechanism of action by inducing aberrant IN multimerization during virion morphogenesis and by competing with IN for binding to its cognate cellular cofactor LEDGF/p75 during early steps of HIV-1 infection. However, quinoline-based ALLINIs impose a low genetic barrier for the evolution of resistant phenotypes, which highlights a need for discovery of second-generation inhibitors. Using crystallographic screening of a library of 971 fragments against the HIV-1 IN catalytic core domain (CCD) followed by a fragment expansion approach, we have identified thiophenecarboxylic acid derivatives that bind at the CCD-CCD dimer interface at the principal lens epithelium-derived growth factor (LEDGF)/p75 binding pocket. The most active derivative (5) inhibited LEDGF/p75-dependent HIV-1 IN activity *in vitro* with an IC$_{50}$ of 72 μM and impaired HIV-1 infection of T cells at an EC$_{50}$ of 36 μM. The identified lead compound, with a relatively small molecular weight (221 Da), provides an optimal building block for developing a new class of inhibitors. Furthermore, although structurally distinct thiophenecarboxylic acid derivatives target a similar pocket at the IN dimer interface as the quinoline-based ALLINIs, the lead compound, 5, inhibited IN mutants that confer resistance to quinoline-based compounds.

Collectively, our findings provide a plausible path for structure-based development of second-generation ALLINIs.

HIV-1 integrase (IN)[3] is the enzyme responsible for the integration of the viral DNA copy of the viral RNA genome into the host chromatin. HIV-1 IN consists of three distinct structural and functional domains: the N-terminal domain, the catalytic core domain (CCD), and the C-terminal domain (1, 2). All three domains contribute to the assembly of the functional stable synaptic complex, where a tetramer of IN is bound to two viral DNA ends (1, 3–7). The cellular chromatin-associated protein lens epithelium-derived growth factor (LEDGF/p75) binds the IN tetramer and facilitates integration of viral DNA into active genes (8–11). The CCD contains several functional determinants of the retroviral enzyme including the DDE catalytic triad, which mediates the catalysis of both 3′-processing and strand transfer reactions. Furthermore, the V-shaped pocket at the CCD-CCD dimer interface provides the principal binding site for the integrase binding domain (IBD) of LEDGF/p75 (12). Therefore, the CCD is an attractive target for the development of new HIV-1 IN inhibitors.

The current FDA-approved inhibitors, raltegravir, elvitegravir, and dolutegravir, bind near the CCD active site in the presence of viral DNA and impair HIV-1 IN strand transfer activity (13–15). Allosteric IN inhibitors (ALLINIs, also known as LEDGINs, NCINIs, INLAIs, or MINIs) bind away from the active site at the distant CCD-CCD dimer interface in the principal LEDGF/p75 binding pocket (16–22). Consequently, ALLINIs impair HIV-1 IN-LEDGF/p75 binding and induce aberrant higher order multimerization of inactive IN *in vitro* (2, 23). In infected cells, ALLINIs inhibit both early and late steps

---

[3] The abbreviations used are: IN, integrase; CCD, catalytic core domain; ALLINI, allosteric integrase inhibitor; LEDGF, lens epithelium-derived growth factor; IBD, integrase binding domain; HTRF, homogeneous time-resolved fluorescence; SAR, structure-activity relationships; LE, ligand efficiency; MD, molecular dynamics.

of HIV-1 replication but are significantly more potent for inducing aberrant IN multimerization during virus particle maturation, likely due to reduced competition with LEDGF/p75 (20, 24–28).

The development of antiviral compounds targeting the IN-LEDGF/p75 binding interface has been fueled by the crystal structure of the IN CCD in complex with the IBD (12). For example, IBD-derived peptides that bind to the CCD-CCD dimer interface have been shown to induce allosteric IN multimerization, thereby inhibiting its catalytic activity *in vitro* and impairing HIV-1 replication in cell culture (29, 30). Furthermore, *in silico* screening using the CCD-IBD co-crystal structure was one method that led to the identification of quinoline-based ALLINIs (16). Strikingly, prior studies that used IN 3′-processing reactions for high-throughput screening identified essentially identical quinoline-based compounds with antiviral activities (17). The emergence of fragment-based drug discovery, which entails screening of libraries of small molecule compounds (typically <250 Da) using either biophysical techniques or enzymatic assays, has opened a novel avenue for the identification of new inhibitors that bind at the IN-LEDGF/p75 interface (31). Several new chemical classes of IN-LEDGF/p75 inhibitors, including benzylindoles (32, 33), benzodioxole-4-carboxylic acid (34), and 8-hydroxyquinoline (35), have been identified using *in silico* methods coupled with fragment-based approaches using surface plasmon resonance or nuclear magnetic resonance (NMR) spectroscopy as primary screening methods. However, further development of these initial fragment hits was hindered by the lack of structural data.
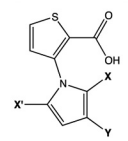
To facilitate structure-based drug design, we have conducted X-ray crystallographic fragment screening, which has led to the identification of new chemical scaffolds that bind to the IN CCD dimer interface at the principal LEDGF/p75 binding site. The optimized derivative impaired recombinant IN activities *in vitro* and inhibited HIV-1 replication in cell culture.
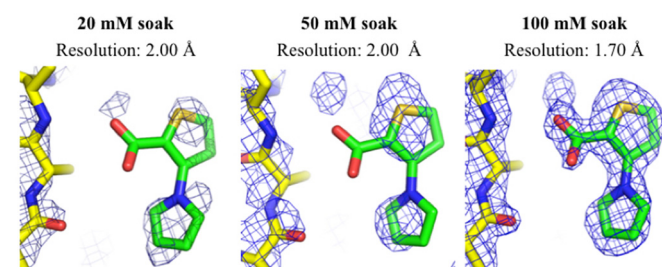
Results and Discussion

Fragment Screening—Crystallographic fragment screening was facilitated by the availability of high resolution IN CCD crystals, which diffract X-rays to 1.8 Å and can be produced within 3 h of setup using the previously described crystallization condition (36). The majority of crystallization drops produced microcrystals with only one of 24 yielding a crystal amenable for small molecule soaking. Subsequent optimization using a combination of pre-seeding and reducing the well volume from 500 μl to 50 μl improved crystal production to approximately 3 suitable crystals per drop. High throughput fragment screening of a chemically diverse library of 971 fragments, consisting of cocktails containing 4–8 compounds each, was conducted using a previously described protocol (37).

Surprisingly, fragment binding for only one mixture soak was observed at the screening concentration of 20 mM (in 20% (v/v) DMSO, the solvent for solubilizing the fragments and a cryoprotectant for freezing crystals). Structure refinement revealed electron density for a fragment bound to a non-biologically relevant pocket formed by crystal contacts. Subsequent hit identification through individual soaking of the mixture components proved to be challenging. Although mixture soaking

TABLE 1
Chemical structures of the compounds and their inhibitory activities in LEDGF/p75-dependent integration assays

	X	X'	Y	Activity (%) at 200 μM	Activity (%) at 400 μM
1	-H	-H	-H	91	83
2	-COH	-H	-H	89	85
3	-COOH	-H	-H	65	45
4	-Cl	-H	-H	81	53
5	-CH₂CH₃	-H	-H	32	1
6	-H	-H	-COH	84	71
7	-H	-H	-CH₂NHCH₂Ph	81	55
8	-Cl	-Cl	-H	82	68

20 mM soak Resolution: 2.00 Å	50 mM soak Resolution: 2.00 Å	100 mM soak Resolution: 1.70 Å

FIGURE 1. **Higher concentration soaks reveal binding of 1 to the LEDGF/p75 binding site at the CCD dimer interface.** Stronger electron density for **1** bound at the LEDGF/p75 site ($2F_o − F_c$ map, contoured at 1.0σ) was observed with increasing concentration.

consistently showed positive electron density, individual fragment soaking at 20 mM failed to reveal fragment-specific electron density. When soaked individually at 50 mM, only one fragment, **1** (Table 1), from the selected mixture displayed binding not only to the previously identified crystal contact site but also revealed weak electron density at the CCD-CCD dimer interface at the principal LEDGF/p75 binding site (Fig. 1). The presence of strong electron density for fragment binding to both sites was confirmed by a 100 mM soak of **1** (Fig. 2, *left*). High concentration screening is not unusual with fragment screening because fragments, due to their small size, tend to have low affinity interactions. In addition, screening with X-ray crystallography often requires higher concentrations due to issues with solubility and occupancy to detect binding (38).

At the LEDGF/p75 binding pocket (Fig. 2, *right*), on monomer A, the carboxylate of fragment **1** forms a direct hydrogen bond with the backbone of Ala-169, whereas two water molecules bridge its interaction with Gln-168. Glu-170, His-171, and Thr-174, the latter of which is also in close contact with the thiophene ring. Relative to the apo structure, the Met-178 side chain rotates into the cavity to establish hydrophobic interactions with the pyrrole ring of **1**. Similarly, on the monomer B, the Gln-95, Trp-132, and Leu-102 side chains rotated by ~170°, ~30°, and ~90°, respectively, establish further hydrophobic interactions with the pyrrole ring. Other hydrophobic interactions mediated via monomer B involve Ala-89, Phe-99, Thr-125, Ala-128, and Ala-129.

Fragment Derivatization—A fragment expansion approach was undertaken to probe structure-activity relationships (SAR) between the lead fragment and the IN CCD. Modification of the pyrrole ring was determined as an ideal starting point for frag-
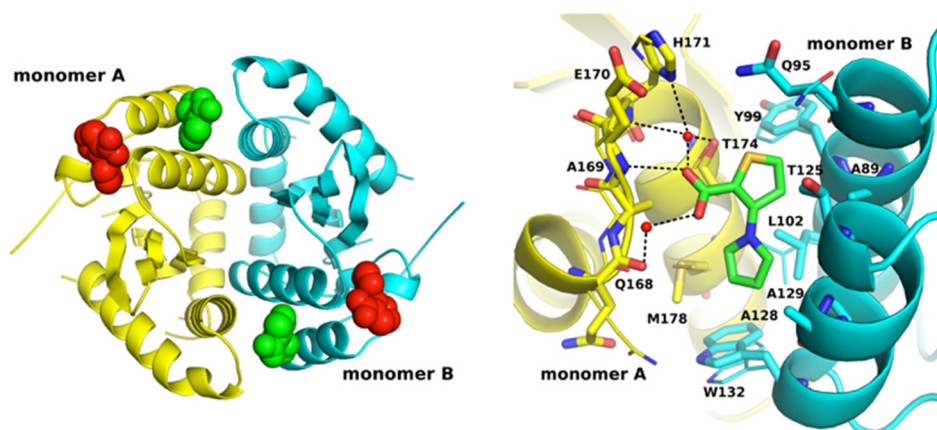
FIGURE 2. **Crystal structure of 1 bound to the IN CCD dimer.** *Left*, crystal structure of **1** bound to a crystal contact site (*red spheres*) and the LEDGF/p75 binding site (*green spheres*) within the IN CCD dimer (*yellow* and *cyan ribbons*, PDB code 5KRS). *Right*, detailed view of **1** (*green*) bound to the LEDGF/p75 binding site. Monomers are shown as *yellow* and *cyan* ribbons; residues defining the binding site are shown as *sticks* (*thin sticks*, apo residue conformations); the bridging water molecules are shown as *red spheres*. *Dashed lines* represent hydrogen bonds (*black*).

ment growth based on the superposition of crystal structures for the fragment hit and available ALLINIs (data not shown). With this in mind, a small series of two- and three-substituted pyrrole analogs (labeled X and Y in Table 1) were designed and synthesized. The two-substituted analogs were prepared via direct halogenation (**4** and **8**) or formylation (**2**, **3**, and **5**) and subsequent functionalization of the ester derivative of fragment **1,** *e.g.* methyl 3-(1H-pyrrol-1-yl)thiophene-2-carboxylate (supplemental information). The preparation of 3-substituted analogs proved to be slightly more challenging due to the inherent preference of pyrroles to react with electrophiles at the 2- rather than the 3-position. To overcome this reactivity, the 3-formyl derivative **6** could be synthesized via Paal-Knorr synthesis (39) from commercially available 2,5-dimethoxytetrahydro-3-furancarbaldehyde and subsequent saponification. This approach also facilitated the preparation of amine **7**.

Biochemical Characterization—A LEDGF/p75-dependent *in vitro* integration assay was used for initial screening of the eight compounds (Table 1). Electron-withdrawing substituents, such as aldehyde and carboxylic acid, at the X position of the pyrrole ring slightly improved potency, whereas the substitution with an ethyl at the same position (**5**) led to near complete inhibition of LEDGF/p75-mediated IN enzymatic activity at the test concentration of 400 μM. Based on these results our future experiments have focused on analyzing **5**. To better understand the SAR, we also examined its less potent analogs **1** and **8** in parallel experiments.

To dissect the mode of action of selected compounds *in vitro*, we examined their ability to inhibit LEDGF/p75-dependent and -independent IN activities as well as to induce aberrant IN multimerization and interfere with IN binding with LEDGF/p75 (Fig. 3, *A*, *B*, *C*, and *D*). Consistent with the initial results in Table 1, Fig. 3, *A* and *D*, show that compound **5** was significantly more potent (IC$_{50}$ of 72 μM) than **8** (IC$_{50}$ >600 μM) or **1** (IC$_{50}$ >800 μM) for inhibiting integration in the LEDGF/p75-dependent assay. The ligand efficiency (LE) for compound **5** was calculated to be 0.38 kcal/mol per non-hydrogen atom (40, 41). This compares favorably to the LE of 0.31 kcal/mol per non-hydrogen atom for direct binding of a highly potent representative ALLINI, BI-D, to IN (42). The inhibition of LEDGF/

p75-dependent activity could be due to (i) compound-induced aberrant protein multimerization of IN resulting in inactivation, (ii) the compound competing with IN binding to LEDGF/p75, or (iii) a combination of these activities. Therefore, a FRET-based IN multimerization assay was used next to help elucidate the mechanism of action for these compounds. In Fig. 3, *B* and *C* (zoomed-in portion of Fig. 3*B*), the multimerization assay shows dose-dependent increases in homogeneous time-resolved fluorescence (HTRF) signal with the addition of **5** or **8** but not for parental compound **1**. However, the extent of HTRF signal increase for these compounds was markedly smaller than that of BI-D, a relatively potent quinoline-based ALLINI (Fig. 3*B*). Higher HTRF counts are indicative of higher order multimerization of IN due to increasing numbers of individual subunits, which are labeled with either donor or acceptor fluorophores, gathering together within the inhibitor-promoted complex. Therefore, the results in Fig. 3*B* suggest that the compounds induced a limited extent of higher order IN multimerization compared with their BI-D counterpart. However, the EC$_{50}$ value of ~26 μM for **5** in the IN multimerization assay correlated well with the IC$_{50}$ value of 60 μM in a LEDGF/p75-independent integration assay (Fig. 3*D*), suggesting that the relatively limited multimerization of IN in the presence of **5** was still sufficient to inhibit IN activity in the absence of LEDGF/p75.

Finally, to examine if the derivatives could also compete with IN-LEDGF/p75 binding, direct binding assays were performed. In addition to promoting aberrant multimerization, **5** inhibited IN binding to LEDGF/p75 with an IC$_{50}$ value of 241 μM (Fig. 3*D*). Overall these results indicate that **5** inhibits IN through a multimodal mechanism of action *in vitro* similar to other quinoline-based ALLINIs such as BI-D.

We next examined the inhibitory activities of **5** with respect to two IN mutants, A128T and H171T, that emerge under the selective genetic pressure of archetypal ALLINI BI-1001 and its more potent analog BI-D, respectively (43, 44). As shown in Fig. 3*E*, **5** inhibited LEDGF/p75-dependent activities of wild-type, H171T, and A128T INs with very similar IC$_{50}$ values. These results indicate that these mutant INs, which were markedly resistant to their respective ALLINIs, were as susceptible to **5** as
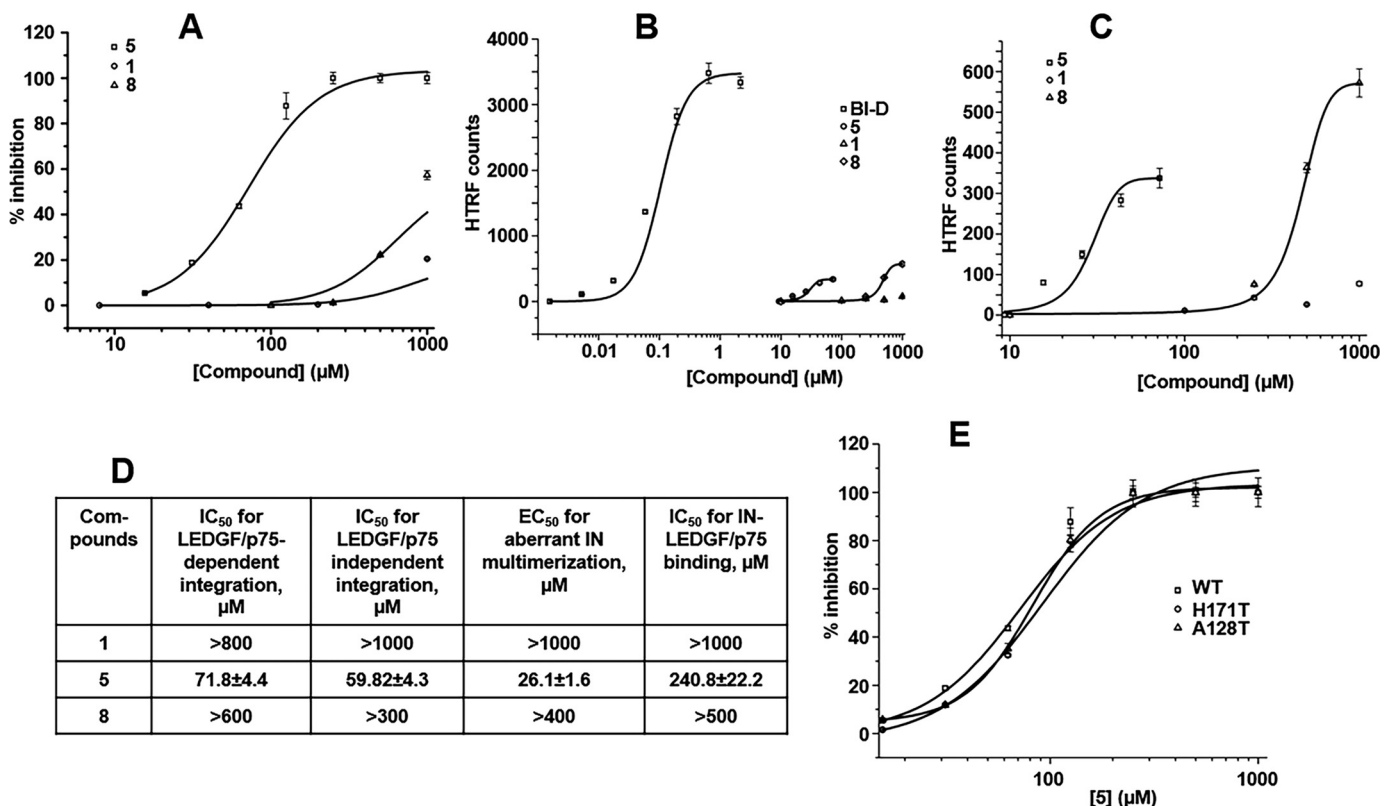
FIGURE 3. *In vitro* **inhibitory activities of compounds 1, 5, and 8.** *A*, dose-dependent effects of the indicated compounds on LEDGF/p75-dependent integration assay. *B*, comparative effects of the indicated fragments and ALLINI BI-D on inducing aberrant IN multimerization. *C*, zoomed-in view of the results in *B* showing the dose-dependent effects of the indicated fragments on promoting higher-order IN multimerization. *D*, summary of inhibitory potencies of the fragments in indicated HTRF-based assays. *E*, inhibitory activities of *5* in LEDGF/p75-dependent integration assays catalyzed by wild-type, A128T, and H171T INs.

the wild-type enzyme. Collectively, our results indicate that **5** is an attractive building block for further development as a second generation ALLINI.

Antiviral Activities—Compound **5** was subsequently tested for antiviral activity during both early and late phases of HIV-1 replication. To determine the activities of **5** during the early phase, SupT1 T cells treated with scale doses of **5** or BI-D, respectively, were infected with a single-round luciferase reporter construct based on HIV-1$_{NL4-3}$ (HIV-Luc), and 2 days later cells were harvested and processed for luciferase assays. Expectedly (24), the EC$_{50}$ of BI-D was 1.2 μM. Rather impressively, **5** had an EC$_{50}$ of 36 μM under these infection conditions (Fig. 4*A*). To determine activities of **5** during the late phase, HIV-Luc was produced in HEK293T cells that were treated with log-scale compound doses. Subsequent infections of SupT1 cells proceeded in the absence of any additional drug in the T cell cultures. As expected (24), BI-D was significantly more potent under these conditions, yielding an EC$_{50}$ of 57 nM (Fig. 4*B*). By contrast, **5** was a few-fold less potent (EC$_{50}$ of 103 μM) as compared with T cells that were directly treated. Unlike previously characterized ALLINIs, these data show that **5** inhibits the early phase of HIV-1 infection more potently than the late phase during HIV-1 particle production. **5** was somewhat more cytotoxic to SupT1 cells than BI-D (520 μM *versus* 175 μM; Fig. 4*C*), yielding a selectivity index of 14.4 during acute HIV-1 infection (Fig. 4*C*).

Structural Characterization—To better understand the SAR of the investigated compounds, crystal-soaking experiments were performed to determine the binding sites of **8** and **5**. A 100 mM soak of **8** with apoCCD crystals showed binding to the two sites identified with **1** (crystal contact and LEDGF/p75 binding sites). Surprisingly, the binding mode of the dual ring system of fragment **8** was flipped (Fig. 5*A*). Compared with **1**, the carboxylate of **8** is involved in a tighter hydrogen bond interaction network with CCD monomer A residues via the backbone amides of Glu-170 and His-171 and the side chains of His-171 and Thr-174. The side chain of Glu-170 formed an additional halogen bonding interaction with one of the chlorine atoms on the pyrrole ring of **8**. Additionally, the aromatic ring system participated in a hydrophobic interaction network formed by residues Met-178 and Ala-169 on CCD monomer A and residues Ala-89, Gln-95, Tyr-99, Leu-102, Thr-125, Ala-128, and Ala-129 on CCD monomer B.

Docking—The most potent compound, fragment **5**, was not amenable to X-ray crystallography. Therefore, we used Auto-Dock4 (45) to predict the binding mode of this fragment. Docking with the hydrated docking protocol (46) revealed **5** binds in a manner similar to **8**. As shown in Fig. 5*B*, the docked binding mode of **5** was predicted to maintain the hydrogen bonds on CCD monomer A with the backbone amides of Glu-170 and His-171 and the side chain of His-171 and Thr-174. The hydrated protocol also predicted a water molecule bridging the
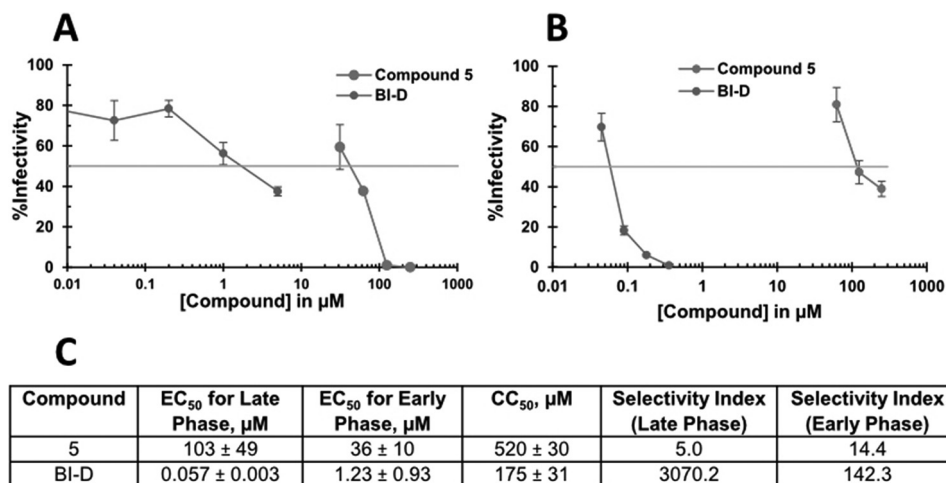
FIGURE 4. *A*, BI-D and compound **5** dose-response curves in treated SupT1 cells (acute or early phase of HIV-1 replication). *B*, HEK293T cells producing HIV-Luc were treated with the indicated concentrations of compounds. Luciferase assays were conducted using SupT1 cell extracts 2 days after HIV-Luc infection. *C*, tabulation of EC_{50} values under the different conditions of HIV-1 infection and CC_{50} values for compound cytotoxicity, as determined by WST-1 cellular proliferation assay.
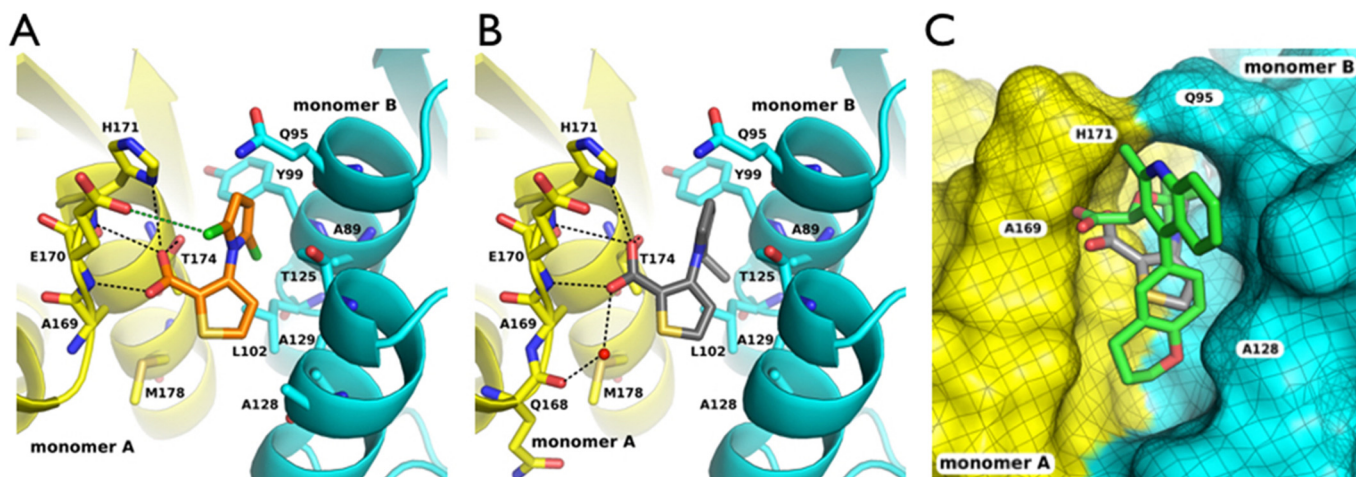

FIGURE 5. *A*, crystallographic structure of **8** bound to IN CCD dimer (PDB code 5KRT). *Dashed lines* represent hydrogen (*black*) and halogen (*green*) bonding interactions. *B*, hydrated docking result of **5** bound to PDB: 5KRS; *dashed lines* represent hydrogen (*black*) bond interactions. *C*, overlay of the crystal structure of BI-D (PDB code 4IDL, *green*) and docked pose of **5** (*gray*) bound to the IN CCD dimer (*yellow*, monomer A; *cyan*, monomer B).

interaction of the carboxylate group with the backbone of Gln-168 on CCD monomer A. This water matches the density of an experimental water at low σ contours present when fragments **1** (Fig. 2, *right*) or **8** is bound (and a similar water found in the BI-D-bound structure; PDB code 4TSX). The ethyl-substituted pyrrole ring of **5** engages a hydrophobic cavity delineated by Thr-174 on CCD monomer A and Ala-89, Tyr-99, Leu-102, and Ala-129 on CCD monomer B. The thiophene of **5** overlaps with the experimentally determined position of the thiophene of **8**, resulting in identical hydrophobic interactions.

To better understand the structural basis for the ability of **5** to inhibit A128T and H171T INs, which confer resistance to certain quinoline-based ALLINIs, binding free energy simulations were performed. The calculated K_d value of 309 μM for **5** binding to the wild-type CCD-CCD (Table 2) was comparable with experimentally determined IC_{50} values in various *in vitro* assays (Fig. 3*D*). Furthermore, the binding affinity of compound **5** to A128T or H171T CCD was reduced only modestly (<2-fold, Table 2) when compared with wild type. The signifi-

TABLE 2

Calculated binding free energies (ΔG) and predicted dissociation constants (K_d) for compound 5 binding to wild-type A128T, and H171T CCD-CCD dimers

SD, standard deviation.

	Wild type	H171T	A128T
$\Delta G \pm SD$ (kcal/mol)	-4.79 ± 0.29	-4.46 ± 0.38	-4.40 ± 0.14
K_d (μM)	309	548	606

cantly smaller size of **5** avoids the steric and electrostatic repulsion effects seen upon binding of BI-1001 to the A128T mutant (43). The reason as to why H171T substitution has little effect on the binding affinity of **5** could be explained by the absence of the *tert*-butoxy moiety in this compound. The *tert*-butoxy group in BI-D hydrogen bonds with Nδ-H of the His-171 side chain and the substitution of this amino acid by Thr reduces binding affinity by ~65-fold (44).

The ability of **5** to inhibit LEDGF/p75 binding to IN could be explained by the significant overlap in the binding interactions between **5** and LEDGF/p75 when bound to the CCD-CCD

TABLE 3
X-ray data and refinement statistics
rmsd, root mean square deviation.

	5KRS	5KRT
PDB accession code	5KRS	5KRT
Compound	**1**	**8**
X-ray source	CHESS F1	CHESS F1
Wavelength (Å)	0.917	0.917
Space group	P3$_1$21	P3$_1$21
Cell constants (*a*, *b*, *c* in Å)	71.91, 71.91, 67.68	72.07, 72.07, 66.35
Resolution range (last shell) (Å)	50.00-1.70 (1.73-1.70)	50.00-1.65 (1.68-1.65)
Completeness (last shell) (%)	98.5 (99.7)	99.5 (100.0)
R$_{merge}$ (last shell)	0.078 (0.646)	0.067 (0.858)
Average I/s (*I*) (last shell)	16.77 (1.83)	29.55 (2.45)
σ cut-off (*I*)	$|I| < -3.0\sigma$	$|I| < -3.0\sigma$
Refinement statistics		
Total no. of atoms (solvent atoms)	2,509 (137)	2,424 (105)
Resolution (Å)	1.70	1.65
No. of reflections (R$_{free}$ set)	22,337 (1,908)	24,261 (1,997)
Completeness (R$_{free}$ set)	98.50 (8.99)	99.54 (8.23)
R$_{work}$	0.173	0.185
R$_{free}$	0.188	0.195
Ramachandran statistics (% of residues in favored/disallowed regions)	98.6/0.0	99.29/0.0
rmsd bond length (Å)	0.005	0.008
rmsd bond angles (°)	0.860	1.329

dimer. For example, both the carboxylate of **5** (Fig. 5*B*) and LEDGF/p75 Asp-366 (12) hydrogen bond with backbone amides of Glu-170 and His-171 in monomer A. In addition, the docking results in Fig. 5*B* show that **5** interacts with both subunits of IN, which is consistent with the inhibitor-induced IN multimerization observed *in vitro* (Fig. 3, *B* and *C*). However, the overlay of binding sites of **5** and BI-D with the CCD-CCD dimer (Fig. 5*C*) reveals that the quinoline-based ALLINI establishes more extensive interactions with both subunits interacting deeper in the binding pocket, whereas the smaller compound **5** has relatively limited contacts with both IN subunits. This in turn could explain the differential extents of IN multimerization seen with these compounds (Fig. 3*B*). The robust, aberrant IN multimerization observed with BI-D could allow for the impairment of the proper maturation of virus particles, whereas the limited multimerization induced by **5** may not suffice to significantly alter IN function during virion morphogenesis, thus reducing its potency in the late stage of viral replication.

Conclusion—In summary, we have conducted X-ray crystallography-based fragment screening to identify novel compounds that bind to the CCD of HIV-1 IN. From a library of 971 fragments, X-ray crystallographic screening identified only one compound, **1**, which bound to a crystal contact site. Subsequent soaking of the individual mixture components at high concentrations revealed additional binding at the LEDGF/p75 binding pocket. Although **1** did not detectably inhibit HIV-1 IN activity, the availability of the crystal structure allowed the use of fragment expansion to generate chemical derivatives, including the most active compound **5**, which inhibited LEDGF/p75-dependent HIV-1 integration at the IC$_{50}$ of 72 μM *in vitro* and impaired the acute phase of HIV-1 replication with an EC$_{50}$ of 36 μM. Furthermore, **5** similarly inhibited the activities of wild-type and mutant INs that confer resistance to quinoline-based ALLINIs. These findings coupled with the small size of the identified lead compound (molecular mass of 221 Da) argue strongly for the further development of 3-(1H-pyrrol-1-yl)-2-thiophenecarboxylic acid derivatives as a second generation of ALLINIs.

Experimental Procedures

HIV-1 IN CCD (F185K) Expression, Purification, and Crystallization—The HIV-1 IN CCD (residues 50–212) containing the F185K mutation was expressed and purified as described (36). The protein was concentrated to 5 mg/ml and crystallized using the hanging-drop vapor diffusion method with a crystallization buffer consisting of 100 mM sodium cacodylate pH 6.5, 100 mM ammonium sulfate, 10% (w/v) PEG 8000, and 5 mM DTT. Crystallization drops were prepared using an equal volume of protein and seed stock consisting of microseeds of HIV-1 IN CCD diluted in the crystallization buffer. Crystallization trays were prepared on ice at room temperature and then transferred to 4 °C for storage.

Crystallographic Fragment Screening, Data Collection, and Refinement—Cocktails of 4–8 compounds were used for the initial screening with single compound soaks to verify the bound fragment identity and to rule out cooperative binding. Fragments, dissolved in DMSO, were soaked into crystals at concentrations of 20, 50, and 100 mM, respectively, with a final DMSO concentration of 20% (v/v) for 2 h before flash-freezing in liquid nitrogen. X-ray diffraction data collection was performed at the Cornell High Energy Synchrotron Source (CHESS) F1 beamline and National Synchrotron Light Source (NSLS) beamline X25 and X29. The diffraction data were indexed, processed, scaled, and merged using *HKL2000* (47). Structure refinement was carried out using PHENIX (1.8.2-1309) (48) and COOT (0.7-rev4459) (49) with riding hydrogens present when the X-ray diffraction resolution was ≥1.9 Å (Table 3). Coordinates and structure factors have been deposited in the PDB under the accession codes 5KRS and 5KRT.

In Vitro Activities of Compounds—Reported (18, 50–52) HTRF-based assays were used to determine the activities of the compounds to inhibit LEDGF/p75-dependent and independent IN activity and IN binding to LEDGF/p75 as well as to induce aberrant, higher order oligomerization of IN.

HIV-1 Infection and Compound Cytotoxicity Assays—HEK293T cells were propagated in Dulbecco's modified Eagle's medium supplemented to contain 100 IU penicillin, 100 μg/ml

streptomycin, and 10% heat inactivated fetal bovine serum, whereas SupT1 cells were grown in similarly supplemented RPMI medium. HIV-Luc was produced by cotransfecting HEK293T cells with pNLX.Luc.R-.ΔAvrII (53) and vesicular stomatitis virus G envelope expression vector pCG-VSV-G (54) at a ratio of 9:1 using PolyJet™ transfection reagent (Signa-Gen). Virion concentration in the resulting cell supernatants was determined using a commercial p24 ELISA kit (Advanced Biosciences Laboratories). HIV-1 infection, luciferase assays, and the WST-1 cell proliferation assay to determine compound toxicity were conducted essentially as previously described (24, 55).

Chemical Synthesis—Compounds were prepared using standard synthetic techniques under an argon atmosphere. Purifications were carried out using silica flash column chromatography, and spectral data (^{1}H and ^{13}C NMR, mass spectroscopy, and IR) was obtained to confirm compound identity. Complete experimental details and copies of NMR spectra for compounds **1**-**8** are included in the supplemental information of this manuscript.

Docking—Three-dimensional coordinates of **5** were generated from the SMILES string using OpenBabel (56), whereas receptor coordinates were extracted from the CCD dimer structure with **8** (PDB code 5KRT). Structures were then prepared following the standard preparation protocol (57). Docking was performed using AutoDock4 with the hydrated docking protocol (46), and 100 poses were generated with the default GA search parameters. Clustering analysis (2.0 Å tolerance) resulted in a single cluster, and lowest energy pose was extracted as final result.

Molecular Dynamics (MD) and Free Energy Simulations—Before running binding free energy calculations, the protein-ligand complexes were subject to several stages of equilibration-production MD simulations, starting from a docked structure for compound **5**, for a total of 15 ns with gradually decreasing harmonic restraints. Then, the absolute binding free energies of **5** with respect to the wild-type, A128T, and H171T CCD dimer were calculated using the double decoupling method (58) in explicit solvent (TIP3P; Ref. 59) water model plus counter ions) at 300 K. The proteins were modeled by the Amber ff99SB-ILDN force field (60), and the compounds were described by the Amber GAFF parameters set (61). The partial charges of the ligands were obtained using the AM1-bcc method (62). For absolute binding free energy calculations, the MD simulation at each λ window was performed using the GROMACS (63, 64) version 4.6.4 for 15 ns; the last 10 ns were used for binding free energy calculations.

References

1. Engelman, A., and Cherepanov, P. (2014) Retroviral integrase structure and dna recombination mechanism. *Microbiol. Spectr.* **2,** 1–22
2. Feng, L., Larue, R. C., Slaughter, A., Kessl, J. J., and Kvaratskhelia, M. (2015) HIV-1 integrase multimerization as a therapeutic target. *Curr. Top. Microbiol. Immunol.* **389,** 93–119
3. Cherepanov, P. (2010) Integrase illuminated. *EMBO Rep.* **11,** 328
4. Li, X., Krishnan, L., Cherepanov, P., and Engelman, A. (2011) Structural biology of retroviral DNA integration. *Virology* **411,** 194–205
5. Cherepanov, P., Maertens, G. N., and Hare, S. (2011) Structural insights into the retroviral DNA integration apparatus. *Curr. Opin. Struct. Biol.* **21,** 249–256
6. Engelman, A., and Cherepanov, P. (2012) The structural biology of HIV-1: mechanistic and therapeutic insights. *Nat. Rev. Microbiol.* **10,** 279–290
7. Krishnan, L., and Engelman, A. (2012) Retroviral integrase proteins and HIV-1 DNA integration. *J. Biol. Chem.* **287,** 40858–40866
8. Cherepanov, P., Maertens, G., Proost, P., Devreese, B., Van Beeumen, J., Engelborghs, Y., De Clercq, E., and Debyser, Z. (2003) HIV-1 integrase forms stable tetramers and associates with LEDGF/p75 protein in human cells. *J. Biol. Chem.* **278,** 372–381
9. Ciuffi, A., Llano, M., Poeschla, E., Hoffmann, C., Leipzig, J., Shinn, P., Ecker, J. R., and Bushman, F. (2005) A role for LEDGF/p75 in targeting HIV DNA integration. *Nat. Med.* **11,** 1287–1289
10. Shun, M. C., Raghavendra, N. K., Vandegraaff, N., Daigle, J. E., Hughes, S., Kellam, P., Cherepanov, P., and Engelman, A. (2007) LEDGF/p75 functions downstream from preintegration complex formation to effect gene-specific HIV-1 integration. *Genes Dev.* **21,** 1767–1778
11. Marshall, H. M., Ronen, K., Berry, C., Llano, M., Sutherland, H., Saenz, D., Bickmore, W., Poeschla, E., and Bushman, F. D. (2007) Role of PSIP1/LEDGF/p75 in lentiviral infectivity and integration targeting. *PLoS ONE* **2,** e1340
12. Cherepanov, P., Ambrosio, A. L., Rahman, S., Ellenberger, T., and Engelman, A. (2005) Structural basis for the recognition between HIV-1 integrase and transcriptional coactivator p75. *Proc. Natl. Acad. Sci. U.S.A.* **102,** 17308–17313
13. Summa, V., Petrocchi, A., Bonelli, F., Crescenzi, B., Donghi, M., Ferrara, M., Fiore, F., Gardelli, C., Gonzalez Paz, O., Hazuda, D. J., Jones, P., Kinzel, O., Laufer, R., Monteagudo, E., Muraglia, E., *et al.* (2008) Discovery of raltegravir, a potent, selective orally bioavailable HIV-integrase inhibitor for the treatment of HIV-AIDS infection. *J. Med. Chem.* **51,** 5843–5855
14. van Lunzen, J., Maggiolo, F., Arribas, J. R., Rakhmanova, A., Yeni, P., Young, B., Rockstroh, J. K., Almond, S., Song, I., Brothers, C., and Min, S. (2012) Once daily dolutegravir (S/GSK1349572) in combination therapy in antiretroviral-naive adults with HIV: planned interim 48 week results from SPRING-1, a dose-ranging, randomised, phase 2b trial. *Lancet Infect. Dis.* **12,** 111–118
15. Pandey, K. K. (2014) Critical appraisal of elvitegravir in the treatment of HIV-1/AIDS. *HIV AIDS (Auckl)*, 10.2147/HIV.S39178
16. Christ, F., Voet, A., Marchand, A., Nicolet, S., Desimmie, B. A., Marchand, D., Bardiot, D., Van der Veken, N. J., Van Remoortel, B., Strelkov, S. V., De Maeyer, M., Chaltin, P., and Debyser, Z. (2010) Rational design of small-molecule inhibitors of the LEDGF/p75-integrase interaction and HIV replication. *Nat. Chem. Biol.* **6,** 442–448
17. Fader, L. D., Malenfant, E., Parisien, M., Carson, R., Bilodeau, F., Landry, S., Pesant, M., Brochu, C., Morin, S., Chabot, C., Halmos, T., Bousquet, Y., Bailey, M. D., Kawai, S. H., Coulombe, R., *et al.* (2014) Discovery of BI 224436, a Noncatalytic Site Integrase Inhibitor (NCINI) of HIV-1. *ACS Med. Chem. Lett.* **5,** 422–427
18. Tsiang, M., Jones, G. S., Niedziela-Majka, A., Kan, E., Lansdon, E. B., Huang, W., Hung, M., Samuel, D., Novikov, N., Xu, Y., Mitchell, M., Guo, H., Babaoglu, K., Liu, X., Geleziunas, R., and Sakowicz, R. (2012) New class of HIV-1 integrase (IN) inhibitors with a dual mode of action. *J. Biol. Chem.* **287,** 21189–21203
19. Sharma, A., Slaughter, A., Jena, N., Feng, L., Kessl, J. J., Fadel, H. J., Malani, N., Male, F., Wu, L., Poeschla, E., Bushman, F. D., Fuchs, J. R., and Kvaratskhelia, M. (2014) A new class of multimerization selective inhibitors of HIV-1 integrase. *PLoS Pathog.* **10,** e1004171

20. Le Rouzic, E., Bonnard, D., Chasset, S., Bruneau, J. M., Chevreuil, F., Le Strat, F., Nguyen, J., Beauvoir, R., Amadori, C., Brias, J., Vomscheid, S., Eiler, S., Lévy, N., Delelis, O., Deprez, E., *et al.* (2013) Dual inhibition of HIV-1 replication by integrase-LEDGF allosteric inhibitors is predominant at the post-integration stage. *Retrovirology* **10,** 144

21. van Bel, N., van der Velden, Y., Bonnard, D., Le Rouzic, E., Das, A. T., Benarous, R., and Berkhout, B. (2014) The allosteric HIV-1 integrase inhibitor BI-D affects virion maturation but does not influence packaging of a functional RNA genome. *PLoS ONE* **9,** e103552

22. Gupta, K., Brady, T., Dyer, B. M., Malani, N., Hwang, Y., Male, F., Nolte, R. T., Wang, L., Velthuisen, E., Jeffrey, J., Van Duyne, G. D., and Bushman, F. D. (2014) Allosteric Inhibition of Human immunodeficiency virus integrase: late block during viral replication and abnormal multimerization involving specific protein domains. *J. Biol. Chem.* **289,** 20477–20488

23. Jurado, K. A., and Engelman, A. (2013) Multimodal mechanism of action of allosteric HIV-1 integrase inhibitors. *Expert Rev. Mol. Med.* **15,** e14

24. Jurado, K. A., Wang, H., Slaughter, A., Feng, L., Kessl, J. J., Koh, Y., Wang, W., Ballandras-Colas, A., Patel, P. A., Fuchs, J. R., Kvaratskhelia, M., and Engelman, A. (2013) Allosteric integrase inhibitor potency is determined through the inhibition of HIV-1 particle maturation. *Proc. Natl. Acad. Sci. U.S.A.* **110,** 8690–8695

25. Balakrishnan, M., Yant, S. R., Tsai, L., O'Sullivan, C., Bam, R. A., Tsai, A., Niedziela-Majka, A., Stray, K. M., Sakowicz, R., and Cihlar, T. (2013) Non-catalytic site HIV-1 integrase inhibitors disrupt core maturation and induce a reverse transcription block in target cells. *PLoS ONE* **8,** e74163

26. Desimmie, B. A., Schrijvers, R., Demeulemeester, J., Borrenberghs, D., Weydert, C., Thys, W., Vets, S., Van Remoortel, B., Hofkens, J., De Rijck, J., Hendrix, J., Bannert, N., Gijsbers, R., Christ, F., and Debyser, Z. (2013) LEDGINs inhibit late stage HIV-1 replication by modulating integrase multimerization in the virions. *Retrovirology* **10,** 57

27. Fontana, J., Jurado, K. A., Cheng, N., Ly, N. L., Fuchs, J. R., Gorelick, R. J., Engelman, A. N., and Steven, A. C. (2015) Distribution and redistribution of HIV-1 nucleocapsid protein in immature, mature, and integrase-inhibited virions: a role for integrase in maturation. *J. Virol.* **89,** 9765–9780

28. Wang, H., Jurado, K. A., Wu, X., Shun, M. C., Li, X., Ferris, A. L., Smith, S. J., Patel, P. A., Fuchs, J. R., Cherepanov, P., Kvaratskhelia, M., Hughes, S. H., and Engelman, A. (2012) HRP2 determines the efficiency and specificity of HIV-1 integration in LEDGF/p75 knockout cells but does not contribute to the antiviral activity of a potent LEDGF/p75-binding site integrase inhibitor. *Nucleic Acids Res.* **40,** 11518–11530

29. Hayouka, Z., Rosenbluh, J., Levin, A., Loya, S., Lebendiker, M., Veprintsev, D., Kotler, M., Hizi, A., Loyter, A., and Friedler, A. (2007) Inhibiting HIV-1 integrase by shifting its oligomerization equilibrium. *Proc. Natl. Acad. Sci. U.S.A.* **104,** 8316–8321

30. Hayouka, Z., Hurevich, M., Levin, A., Benyamini, H., Iosub, A., Maes, M., Shalev, D. E., Loyter, A., Gilon, C., and Friedler, A. (2010) Cyclic peptide inhibitors of HIV-1 integrase derived from the LEDGF/p75 protein. *Bioorg. Med. Chem.* **18,** 8388–8395

31. Hajduk, P. J., and Greer, J. (2007) A decade of fragment-based drug design: strategic advances and lessons learned. *Nat. Rev. Drug Discov.* **6,** 211–219

32. De Luca, L., Barreca, M. L., Ferro, S., Christ, F., Iraci, N., Gitto, R., Monforte, A. M., Debyser, Z., and Chimirri, A. (2009) Pharmacophore-based discovery of small-molecule inhibitors of protein-protein interactions between HIV-1 integrase and cellular cofactor LEDGF/p75. *Chem. Med. Chem.* **4,** 1311–1316

33. De Luca, L., Ferro, S., Gitto, R., Barreca, M. L., Agnello, S., Christ, F., Debyser, Z., and Chimirri, A. (2010) Small molecules targeting the interaction between HIV-1 integrase and LEDGF/p75 cofactor. *Bioorg. Med. Chem.* **18,** 7515–7521

34. Peat, T. S., Rhodes, D. I., Vandegraaff, N., Le, G., Smith, J. A., Clark, L. J., Jones, E. D., Coates, J. A., Thienthong, N., Newman, J., Dolezal, O., Mulder, R., Ryan, J. H., Savage, G. P., Francis, C. L., and Deadman, J. J. (2012) Small molecule inhibitors of the LEDGF site of human immunodeficiency virus integrase identified by fragment screening and structure based design. *PLoS ONE* **7,** e40147

35. Serrao, E., Debnath, B., Otake, H., Kuang, Y., Christ, F., Debyser, Z., and Neamati, N. (2013) Fragment-based discovery of 8-hydroxyquinoline inhibitors of the HIV-1 integrase-lens epithelium-derived growth factor/p75 (IN-LEDGF/p75) interaction. *J. Med. Chem.* **56,** 2311–2322

36. Dyda, F., Hickman, A. B., Jenkins, T. M., Engelman, A., Craigie, R., and Davies, D. R. (1994) Crystal structure of the catalytic domain of HIV-1 integrase: similarity to other polynucleotidyltransferases. *Science* **266,** 1981–1986

37. Bauman, J. D., Patel, D., Dharia, C., Fromer, M. W., Ahmed, S., Frenkel, Y., Vijayan, R. S., Eck, J. T., Ho, W. C., Das, K., Shatkin, A. J., and Arnold, E. (2013) Detecting allosteric sites of HIV-1 reverse transcriptase by X-ray crystallographic fragment screening. *J. Med. Chem.* **56,** 2738–2746

38. Patel, D., Bauman, J. D., and Arnold, E. (2014) Advantages of crystallographic fragment screening: functional and mechanistic insights from a powerful platform for efficient drug discovery. *Prog. Biophys. Mol. Biol.* **116,** 92–100

39. Rault, S., Lancelot, J. C., Prunier, H., Robba, M., Renard, P., Delagrange, P., Pfeiffer, B., Caignard, D. H., Guardiola-Lemaitre, B., and Hamon, M. (1996) Novel selective and partial agonists of 5-HT3 receptors. Part 1. Synthesis and biological evaluation of piperazinopyrrolothienopyrazines. *J. Med. Chem.* **39,** 2068–2080

40. Kuntz, I. D., Chen, K., Sharp, K. A., and Kollman, P. A. (1999) The maximal affinity of ligands. *Proc. Natl. Acad. Sci. U.S.A.* **96,** 9997–10002

41. Hopkins, A. L., Groom, C. R., and Alex, A. (2004) Ligand efficiency: a useful metric for lead selection. *Drug Discov. Today* **9,** 430–431

42. Feng, L., Dharmarajan, V., Serrao, E., Hoyte, A., Larue, R. C., Slaughter, A., Sharma, A., Plumb, M. R., Kessl, J. J., Fuchs, J. R., Bushman, F. D., Engelman, A. N., Griffin, P. R., and Kvaratskhelia, M. (2016) The competitive Interplay between allosteric HIV-1 integrase inhibitor BI/D and LEDGF/p75 during the early stage of HIV-1 replication adversely affects inhibitor potency. *ACS Chem. Biol.* **11,** 1313–1321

43. Feng, L., Sharma, A., Slaughter, A., Jena, N., Koh, Y., Shkriabai, N., Larue, R. C., Patel, P. A., Mitsuya, H., Kessl, J. J., Engelman, A., Fuchs, J. R., and Kvaratskhelia, M. (2013) The A128T resistance mutation reveals aberrant protein multimerization as the primary mechanism of action of allosteric HIV-1 integrase inhibitors. *J. Biol. Chem.* **288,** 15813–15820

44. Slaughter, A., Jurado, K. A., Deng, N., Feng, L., Kessl, J. J., Shkriabai, N., Larue, R. C., Fadel, H. J., Patel, P. A., Jena, N., Fuchs, J. R., Poeschla, E., Levy, R. M., Engelman, A., and Kvaratskhelia, M. (2014) The mechanism of H171T resistance reveals the importance of N inverted question mark-protonated His-171 for the binding of allosteric inhibitor BI-D to HIV-1 integrase. *Retrovirology* **11,** 100

45. Morris, G. M., Huey, R., Lindstrom, W., Sanner, M. F., Belew, R. K., Goodsell, D. S., and Olson, A. J. (2009) AutoDock4 and AutoDockTools4: automated docking with selective receptor flexibility. *J. Comput. Chem.* **30,** 2785–2791

46. Forli, S., and Olson, A. J. (2012) A force field with discrete displaceable waters and desolvation entropy for hydrated ligand docking. *J. Med. Chem.* **55,** 623–638

47. Otwinowski, Z., Borek, M. W. D., and Cymborowski, M. (2011) DENZO and SCALEPACK. in *International Tables for Crystallography* (Arnold, E., Himmel, D. M., and Rossmann, M. G., ed.) pp. 226–235, John Wiley & Sons, West Sussex, UK

48. Adams, P. D., Afonine, P. V., Bunkóczi, G., Chen, V. B., Davis, I. W., Echols, N., Headd, J. J., Hung, L. W., Kapral, G. J., Grosse-Kunstleve, R. W., McCoy, A. J., Moriarty, N. W., Oeffner, R., Read, R. J., Richardson, D. C., Richardson, J. S., Terwilliger, T. C., and Zwart, P. H. (2010) PHENIX: a comprehensive Python-based system for macromolecular structure solution. *Acta Crystallogr. D. Biol. Crystallogr.* **66,** 213–221

49. Emsley, P., Lohkamp, B., Scott, W. G., and Cowtan, K. (2010) Features and development of Coot. *Acta Crystallogr. D. Biol. Crystallogr.* **66,** 486–501

50. Wang, Y., Klock, H., Yin, H., Wolff, K., Bieza, K., Niswonger, K., Matzen, J., Gunderson, D., Hale, J., Lesley, S., Kuhen, K., Caldwell, J., and Brinker, A. (2005) Homogeneous high-throughput screening assays for HIV-1 integrase 3β-processing and strand transfer activities. *J. Biomol. Screen.* **10,** 456–462

51. Kessl, J. J., Jena, N., Koh, Y., Taskent-Sezgin, H., Slaughter, A., Feng, L., de Silva, S., Wu, L., Le Grice, S. F., Engelman, A., Fuchs, J. R., and Kvaratskhe-

lia, M. (2012) A multimode, cooperative mechanism of action of allosteric HIV-1 integrase inhibitors. *J. Biol. Chem.* **287,** 16801–16811

52. Kessl, J. J., Sharma, A., and Kvaratskhelia, M. (2016) Methods for the analyses of inhibitor-induced aberrant multimerization of HIV-1 integrase. *Methods Mol. Biol.* **1354,** 149–164

53. Koh, Y., Wu, X., Ferris, A. L., Matreyek, K. A., Smith, S. J., Lee, K., Kewal-Ramani, V. N., Hughes, S. H., and Engelman, A. (2013) Differential effects of human immunodeficiency virus type 1 capsid and cellular factors nucleoporin 153 and LEDGF/p75 on the efficiency and specificity of viral DNA integration. *J. Virol.* **87,** 648–658

54. Shun, M. C., Daigle, J. E., Vandegraaff, N., and Engelman, A. (2007) Wild-type levels of human immunodeficiency virus type 1 infectivity in the absence of cellular emerin protein. *J. Virol.* **81,** 166–172

55. Sowd, G. A., Serrao, E., Wang, H., Wang, W., Fadel, H. J., Poeschla, E. M., and Engelman, A. N. (2016) A critical role for alternative polyadenylation factor CPSF6 in targeting HIV-1 integration to transcriptionally active chromatin. *Proc. Natl. Acad. Sci. U.S.A.* **113,** E1054–E1063

56. O'Boyle, N. M., Banck, M., James, C. A., Morley, C., Vandermeersch, T., and Hutchison, G. R. (2011) Open Babel: An open chemical toolbox. *J. Cheminform.* **3,** 33

57. Forli, S., Huey, R., Pique, M. E., Sanner, M. F., Goodsell, D. S., and Olson, A. J. (2016) Computational protein-ligand docking and virtual drug screening with the AutoDock suite. *Nat. Protoc.* **11,** 905–919

58. Deng, N. J., Zhang, P., Cieplak, P., and Lai, L. (2011) Elucidating the energetics of entropically driven protein-ligand association: calculations of absolute binding free energy and entropy. *J. Phys. Chem. B.* **115,** 11902–11910

59. Jorgensen, W. L., Chandrasekhar, J., Madura, J. D., Impey, R. W., and Klein, M. L. (1983) Comparison of simple potential functions for simulating liquid water. *J. Chem. Phys.* **79,** 926–935

60. Lindorff-Larsen, K., Piana, S., Palmo, K., Maragakis, P., Klepeis, J. L., Dror, R. O., and Shaw, D. E. (2010) Improved side-chain torsion potentials for the Amber ff99SB protein force field. *Proteins* **78,** 1950–1958

61. Wang, J., Wolf, R. M., Caldwell, J. W., Kollman, P. A., and Case, D. A. (2004) Development and testing of a general amber force field. *J. Comput. Chem.* **25,** 1157–1174

62. Jakalian, A., Jack, D. B., and Bayly, C. I. (2002) Fast, efficient generation of high-quality atomic charges. AM1-BCC model: II. Parameterization and validation. *J. Comput Chem.* **23,** 1623–1641

63. Hess, B., Kutzner, C., van der Spoel, D., and Lindahl, E. (2008) GROMACS 4: algorithms for highly efficient, load-balanced, and scalable molecular simulation. *J. Chem. Theory Comput.* **4,** 435–447

64. Pronk, S., Páll, S., Schulz, R., Larsson, P., Bjelkmar, P., Apostolov, R., Shirts, M. R., Smith, J. C., Kasson, P. M., van der Spoel, D., Hess, B., and Lindahl, E. (2013) GROMACS 4.5: a high-throughput and highly parallel open source molecular simulation toolkit. *Bioinformatics* **29,** 845–854

Disha Patel, Janet Antwi, Pratibha C. Koneru, Erik Serrao, Stefano Forli, Jacques J. Kessl, Lei Feng, Nanjie Deng, Ronald M. Levy, James R. Fuchs, Arthur J. Olson, Alan N. Engelman, Joseph D. Bauman, Mamuka Kvaratskhelia and Eddy Arnold

Access the most updated version of this article at doi: 10.1074/jbc.M116.753384

Alerts:
- When this article is cited
- When a correction for this article is posted

Click here to choose from all of JBC's e-mail alerts

Supplemental material:
http://www.jbc.org/content/suppl/2016/09/19/M116.753384.DC1

This article cites 63 references, 17 of which can be accessed free at
http://www.jbc.org/content/291/45/23569.full.html#ref-list-1